RESEARCH ARTICLE   OPEN ACCESS

Analysis of X-ray peak broadening and determination of nanosizes, microstrains, stresses and energy densities associated with nanoparticles of zinc oxide powders prepared from high energy planetary ball mill technique

D.G.Patil*, S.D.Bagul, P.S.Sonawane,M.S.Wagh, L.A.Patil
Nanomaterials Research Lab, P.G.Department of Physics, Pratap College Amalner 42540, India
Corresponding author: D.G.Patil

ABSTRACT
Nanostructured ZnO powder was prepared using high energy planetary ball mill (Retsch PM 100) technique. Commercially available ZnO powder was used as starting material for milling. Nanocrystalline ZnO powder samples were prepared at different milling conditions such as milling speed, milling time interval, ball to powder weight ratio (BPR) and ball size (20mm, 10mm and 5mm diameters).Efforts were made to optimize milling conditions till smallest possible particle size was obtained. The powders were prepared without using the process control agent (PCA).XRD technique was used to study structural properties of the powders. X ray peak broadening induced due to change in particle size and strain was analyzed using Debye-Scherrer formula and Williamson-Hall (W-H) plots. Microstructural study was conducted using SEM (scanning electron microscopy) technique. The strain, stress and energy density associated with powder particles were determined. The FWHM of major peak (101) from XRD patterns of different the powders were observed to be increasing with decreasing particle size. The results were discussed and interpreted.
Keywords: ZnO, High energy planetary ball mill, X ray peak broadening, Williamson-Hall plots, Size-stress-strain-energy density

I. INTRODUCTION

Zinc oxide (ZnO) is technologically important semiconductor. It has wide band gap energy, (3.37 eV), large exciton binding energy (60 eV)and excellent chemical stability. Zinc oxide can be used in practical applications viz. in gas sensors, ceramics, field-emission devices and luminescent materials [1-3]. It is highly applicable in solar cells, photo catalysis, and chemical sensors [4-11]. Nanoparticles (NPs) have revolutionized major industrial areas, from drug delivery to agriculture and food industry [12]. It is desirable to reduce environmental pollution by replacing chemical methods of synthesis. New methods can overcome the drawbacks of chemical methods, improve the yield, and reduce the cost [13]. Bulk zinc oxide is cost-effective and shows a variety of applications in industry [14-15]. ZnO nanocrystals predominantly show wurtzite structure. ZnO in its simplest form shows tetrahedron geometry which makes it applicable for acoustic wave resonators and acoustic-optic modulators. Nanocrystalline ZnO based sunscreen lotion can protects the skin from ultraviolet radiations. It has also been used in foot care and ointments [16-19]. ZnO is useful agent for bioimaging as it emits green luminescence. ZnO is considered as an important material for its use in the treatment of diseases like hemophilia, chronic granulomatous disorder (CGD), neurodegenerative diseases, genital blindness, diabetes, viral infections and heart disease. It has been reported that ZnO based biosensors are useful for sensing cholesterol, biochemistry of enzymes, and other biosensing applications [20-21]. ZnO can be prepared using various physical and chemical routes. High Energy Ball Milling is one of the important techniques to prepare nanocrystalline ZnO. High Energy Planetary ball mill (referred to as Pulverisette)is popular mill in which a few hundred grams of nanocrystalline ZnO powder can be milled at a time. The planetary ball mill owes its name to the planet-like movement of its vials [22].

Lattice strain or microstrain is a local deviation of interplaner spacings from the average value caused by local defects. X-ray diffraction technique is important to understand the structure of the material. The Scherrer Debye method is used to determine the crystallite size by analyzing major peak of XRD pattern. Different models of Williamson-Hall method[23] are based on analysis of broadening of XRD peaks in full diffraction patterns to calculate the crystallite size, lattice

strain, stress and energy density by analyzing. Crystallite size broadening is proportional to $1/\cos\theta$ and integral breadth of the strain-related diffraction peak broadening is proportional to $\tan\theta$.

II. EXPERIMENTAL

Commercially available ZnO powder was used as starting material. The powder was milled by using high energy planetary ball mill - Retsch PM 100 to obtain monodisperse nanocrystalline ZnO powder. Grinding jar (250 ml) and balls made up of Zirconium Oxide (ZrO_2) were used as grinding medium in high energy planetary ball mill. Different milling experiments were conducted to optimize milling conditions to get smallest possible nanoparticles of ZnO. Nanocrystalline ZnO powder samples were prepared by varying milling conditions, such as, milling speed (200, 300, 400 and 500 rpm), milling time interval (4h, 8h,12h, 24h, 36h, 42h, 48h and 60h), ball to powder weight ratio (BPR3.5:1, 5:1, 10:1, 15:1, 30:1, 37.5:1, 45:1 and 60:1), ball size (20mm, 10mm and 5mm diameters). Milling of powder was conducted with and without adding methanol as process control agent (PCA). One cycle of milling time interval was made up of 70 min. Each milling time cycle of 70 min was bifurcated into: 60 min (milling on) and 10min interval (milling off). Off time interval in milling process was required to normalize the energy evolving and in turn rising of temperature while milling.

The structural properties of the powder were studied using X ray diffraction technique (using Rigaku's MiniFlex 600 Bench top XRD). The X ray peak broadening induced due to reduction in size and due to strain associated with nanoparticles was analyzed using Debye Scherrer and Williamson–Hall (W–H) methods(Uniform Deformation Model (UDM), Uniform Stress Deformation Model (USDM) and Uniform Deformation Energy Density Model (UDEDM)). The microstructural properties of the powder particles were studied using SEM (Hitachi S-4800) and TEM (Philips, model CM 200) images.

III. RESULTSAND DISCUSSION
3.1. Ball milling of ZnO powder to get smallest size of nanoparticles
3.1.1 Milling of ZnO powder at different milling speeds

Milling Experiments were conducted at milling speeds of: 200,300,400 and 500 rpm at ball to powder ratio (BPR) of 15:1, with balls of 10 mm diameter and with milling time interval of 4h. 5 wt % methanol was added as process control agent (PCA) into the grinding jar before start of the milling process.
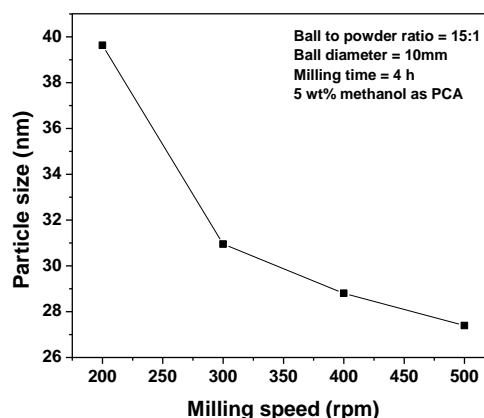

Fig.1 Variation of Particle size with milling speed

The average size of nanoparticles associated with ZnO powder prepared with milling speed of 500 rpm was found to be the smallest. Therefore milling speed of 500 rpm was found to be optimum. But at this milling speed, larger heat was observed to be generated and there was the possibility of agglomeration of smaller particles forming larger particles. Therefore, milling speed of 300 rpm was preferred for further milling process. No considerable difference in sizes of nanoparticles was observed in powders prepared by milling speeds of: 300 rpm and 500 rpm. Soft milling conditions (milling at 300 rpm instead of 500 rpm) were preferred.

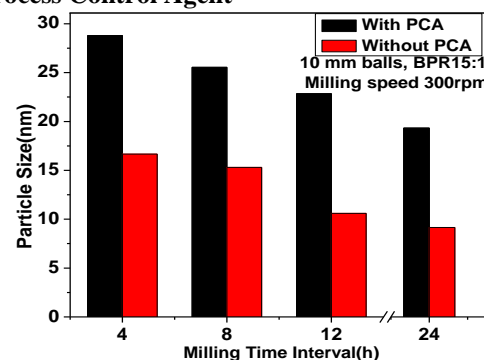### 3.1.2. Milling of ZnO powder with and without Process Control Agent

Fig.2 Milling with and without Process Control Agent

The bar diagram in figure 2 shows the comparison of particle sizes of the powders milled with and without process control agent (PCA). Keeping other milling conditions identical (balls of 10 mm diameter, BPR of 15:1, milling speed of 300rpm), the nanoparticle sizes of the powders milled without PCA were observed to be relatively smaller as compared with the nanoparticle sizes of

respective powders milled with PCA for identical milling conditions.

3.1.3 Milling of ZnO powder using balls of different diameters
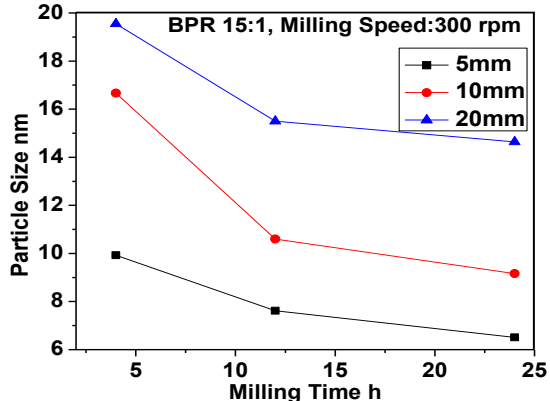

Fig. 3 Variation of particle size with milling time

Nanoparticle size was decreasing with increase in milling time interval for any ball of typical size indicated in figure 3. Smaller the size of ball used for milling smaller the size of nanoparticles obtained for identical milling conditions.

3.1.4. Dependence of size of nanoparticles on BPR (ball to powder ratio) and ball diameter
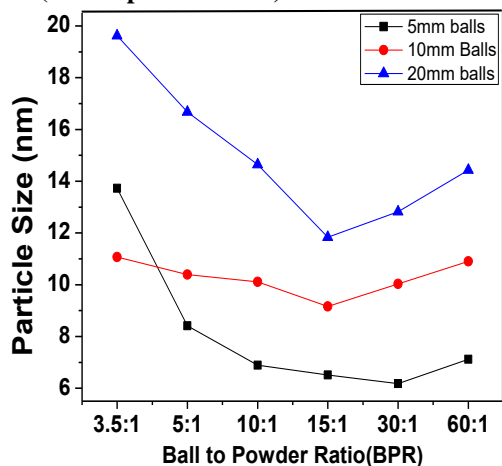

Fig. 4 Variation of ZnO nanoparticle size with ball to powder ratio

Figure4shows variation of size of nanoparticles with the variation of ball to powder ratio when milling time interval was 24h and milling speed was 300rpm.Three graphs in the figure are corresponding to the powders milled by using balls of 5mm, 10mm and 20mmdiameters.

The size of nanoparticle was observed to be decreasing with an increase of BPR, reached to minimum at typical BPR and was then increasing with further increase of BPR. . Optimum BPR was found to be 30:1 when balls of 5mm were used and

was 15:1 when balls of 10mm and 20mm were used for milling of powders. The smallest nanoparticles of average size of 6.2 nm were obtained with balls of 5mm, the smallest nanoparticles of average size of 9.2 nm were obtained with balls of 10mm and the smallest nanoparticles of average size of 11.8nm were obtained with balls of 20mm as calculated by using Scherrer Debye method. For BPR smaller than 5:1, the average size of nanoparticles was observed to be smaller when powder was milled by 10 mm balls as compared to the size of nanoparticles when powder was milled by 5 mm balls.

3.1.5 Variation of size of nanopaticles with variation of milling time intervals
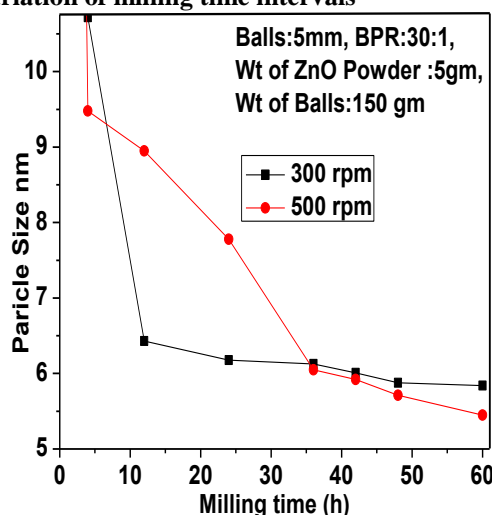

Fig.5 Variation of size of nanoparticles with milling (speeds of 300 and 500 rpm) time interval

The powder milling experiments were conducted at milling speeds of 300 rpm and 500 rpm keeping other milling conditions identical. Particle sizes of powders milled at 300 and 500rpm are decreasing with milling time. Rate of decrement in size of powders particle milled at milling speed of 500rpm was observed to be larger as compared to the powders milled at milling speed of 300rpm as indicated in Figure 5. The rate of reduction in sizes of particles for milling time intervals more than 36 h was relative smaller.

3.1.6 Milling of powder using mixture of balls of different diameters (5mm and 10mm)

Efforts were made to mill the powder using mixture of balls of different diameters (different composition of 5mm and 10 mm balls)with BPR of 15:1, milling speed of 300 rpm and milling time interval of 24h.
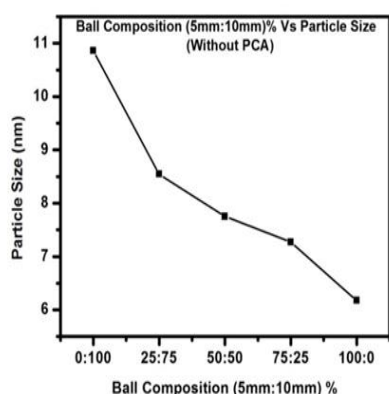
The milling with mixture of balls was not found to be beneficial as compared with the milling with balls of single type to get smallest size of nanoparticles in identical milling conditions. The graph in figure 6 shows that the smallest size of nanoparticles (7.3nm) was possible at 75:25composition of 5mm and 10 mm balls.100:0 composition corresponds to 100% balls of 5mm diameter.

Fig.6 Variation of particle size with variation of compositions of balls of different diameters

3.2Analysis of X-Ray peak broadening
3.2.1(a) X-Ray diffraction patterns of some ball milled powders
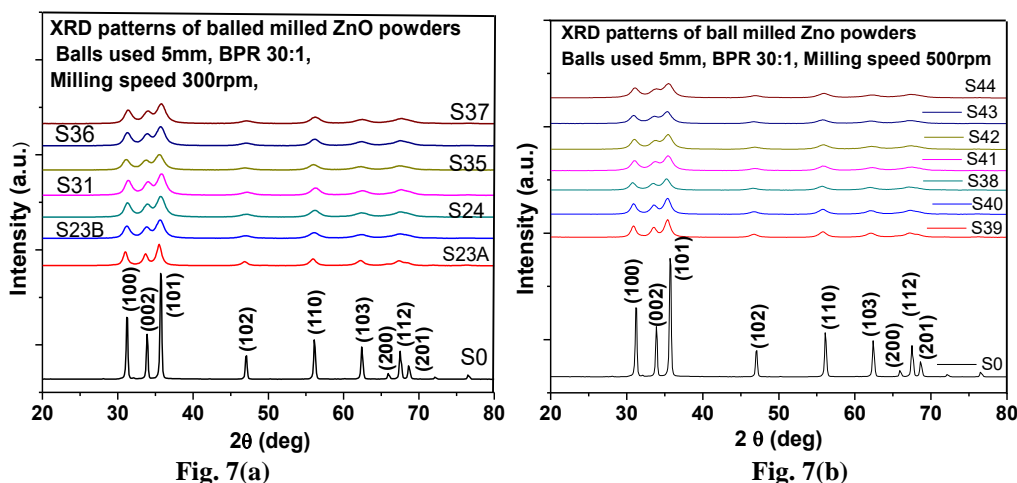

Fig. 7(a)

Fig. 7(b)

Fig.7 XRD patterns of ZnO powders milled at speeds of: (a) 300rpm and (b) 500rpm

The structural analysis of nanostructured ZnO powders was carried out from Rigaku's MiniFlex 600 Bench top XRD Diffractometer (XRD) with CuKα radiation of wavelength of 1.5418 Å. Observed XRD peaks of all samples match exactly with peaks reported in standard JCPDS data (JCPDS 36-1451). The XRD patterns confirmed the powders to be the Wurtzite phase of ZnO. Overlapped XRD patterns of ZnO powder samples presented in figures 7(a) and 7(b) are for comparison of peak broadening. Larger broadening of peaks in XRD pattern was observed for nanoparticles of smaller size. Broadening (FWHM) of major XRD peak (101) of sample S37 or S44 was largest as compared with the broadening of major XRD peaks (101)other balled milled ZnO powder sample.

X-ray diffraction patterns were used to determine the size of nanoparticles and lattice strain by analyzing the broadening of their peaks.

It is clear from Table 1 that FWHM goes on increasing with decrease of size of nanoparticle. Average size of nanoparticles associated with S37 powder is smallest and FWHM is largest. The values of unit cell lattice parameters ('a', 'c' and 'V') of S37 are smaller as compared to the values of unmilled powder S0. c/a values of all samples are almost constant.

Table 1.FWHM, size of nanoparticles and lattice parameters, Milling speed 300rpm

Parameters	5mm Balls, BPR=30:1, Milling speed 300rpm, No PCA						
Sample Name	S23B	S23A	S24	S31	S35	S36	S37
Milling time h	4	12	24	36	42	48	60
2 θ deg.	35.491	35.633	35.711	35.802	35.695	35.510	35.746
d Å for (101)	2.5273	2.5176	2.5122	2.5061	2.5134	2.5260	2.5098
FWHM (deg.)	0.779	1.298	1.35	1.362	1.39	1.42	1.43
Particle Size nm	10.72	6.43	6.178	6.126	6.007	5.876	5.84
d Å for (100)	2.8673	2.8821	2.8586	2.8514	2.8741	2.8592	2.8508
d Å for (002)	2.6463	2.6599	2.6387	2.6330	2.6522	2.6400	2.6336
a Å	3.3109	3.3280	3.3008	3.2925	3.3187	3.3015	3.2918
c Å	5.2926	5.3198	5.2774	5.266	5.3044	5.28	5.2672
c/a	1.5985	1.5985	1.5988	1.5994	1.5983	1.5993	1.6
V Å³	87.03	88.38	86.25	85.63	87.63	86.33	85.61

Table 2.FWHM, size of nanoparticles and lattice parameters, Milling speed 500rpm

Parameters	5mm Balls, BPR=30:1, Milling speed 500rpm, No PCA						
Sample Name	S39	S40	S38	S41	S42	S43	S44
Milling time h	4	12	24	36	42	48	60
2 θ deg.	35.111	35.373	35.392	35.425	35.445	35.297	35.456
d for (101)	2.5538	2.5354	2.5341	2.5319	2.5305	2.5407	2.5297
FWHM (deg.)	0.88	0.932	1.072	1.38	1.41	1.46	1.53
Particle Size nm	9.48	8.95	7.78	6.05	5.92	5.71	5.45
d for (100)	2.8949	2.8926	2.9139	2.8843	2.8956	2.8838	2.8788
d for (002)	2.6689	2.6647	2.689	2.6566	2.6633	2.6546	2.651
a Å	3.3427	3.3401	3.3647	3.3305	3.3436	3.3299	3.3242
c Å	5.3378	5.3294	5.378	5.3132	5.3266	5.3092	5.302
c/a	1.5969	1.5956	1.5984	1.5953	1.5931	1.5944	1.5950
V Å³	89.47	89.18	91.33	88.40	88.32	88.30	87.88

It is clear from Table 2 that FWHM goes on increasing with decrease of size of nanoparticle. Average size of nanoparticles associated with S44 powder is smallest and FWHM is largest. The values of unit cell lattice parameters ('a', 'c' and 'V') of S44 are smaller as compared to the values of unmilled powder S0. The 'c/a' values of all samples are almost constant.

3.2.1(b) Broadening of major peaks (101) in XRD patterns of ZnO powders and variation of particle size
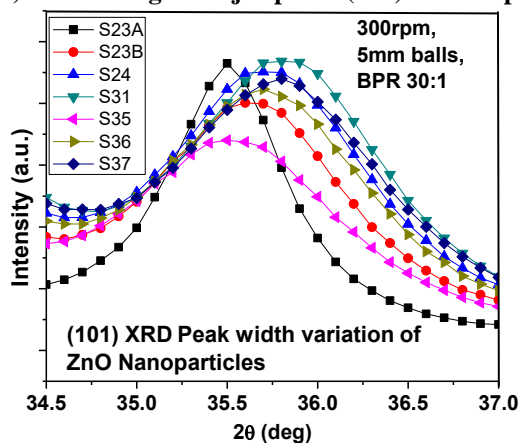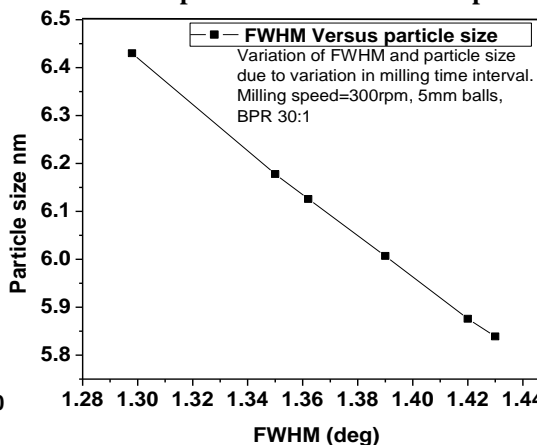

Fig. 8(a) Broadening of peaks (300rpm)　　　　**Fig. 8(b) Variation of FWHM**
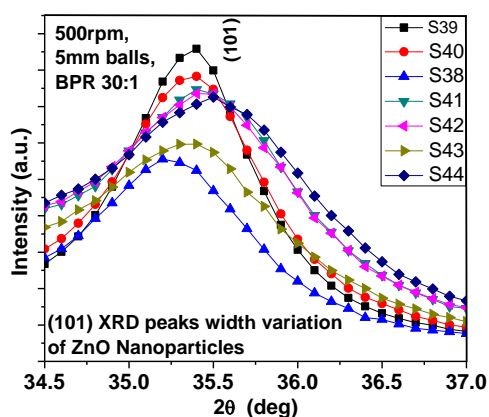
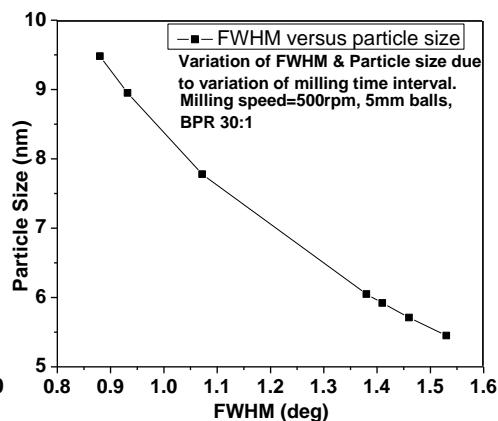**Fig. 8(c)Broadening of peaks (500rpm)**   **Fig. 8(d)Variation of FWHM**

Figure 8. Major XRD peak (101) broadening of powders milled with 300rpm and 500rpm.

Figure 8(a) shows overlapped major XRD peaks of ZnO powders prepared using milling speed of 300rpm.The ZnO- starting material sample-So shows smallest FWHM (β = 0.220º).Its average particle size was found to be largest (38nm) and the balled milled ZnO sample-S37 shows largest FWHM (β = 1.43º- peak broadening).Its average particle size was found to be smallest (5.8nm) as determined by using Debye Scherrer method. The remaining samples shown in Figure 8(a) have particle sizes in between5.8nm and 38nm and in turn FWHM. Figure 8(b) shows decrease of particle size with an increase of FWHM.

Figure 8(c) shows overlapped major XRD peaks of ZnO powders prepared using milling speed of 500rpm. Ball milled ZnO sample-S44 shows largest FWHM (β = 1.53º- peak broadening).Its average particle size was found to be smallest (5.5nm) as determined by using Debye Scherrer method. Figure 8(d) shows decrease of particle size with an increase of FWHM.

3.2.2 Analysis of peak broadening using Debye Scherrer method and W-H plots

XRD patterns show 'peak broadening'. The observed peak broadening may be due to smaller size of nanoparticle and strain induced on particles during milling. Particle size and strain associated with powder particles were calculated by analyzing peak broadening in respective XRD patterns. Debye Scherrer method, W-H plots (Uniform Deformation Model (UDM), Uniform Stress Deformation model (USDM), Uniform Deformation Energy Density Model

(UDEDM)[ ]were used to analyze the crystallite size and strain of S37 and S44 powder samples. SEM images were also used to know size and morphology of the particles.

(a) Determination of particle Size using Debye–Scherrer equation

Average particle size (t), dislocation density (δ) and ZnO bond length (L) of ZnO powder samples S7 and S24 were determined using Debye Scherrer Method and are presented in Table 1.

Average size ZnO nanocrystallites (t) was determined by using Debye–Scherrer equation (1),

$$t = \frac{0.9\lambda}{\beta_{hkl}Cos\theta} \qquad (1)$$

where β_{hkl} is full width at half maximum(FWHM) of major peak in XRD pattern, λ is the wave length of the incident X-ray (λ = 1.5418 Å) and θ is the Bragg angle.

The dislocation density (δ) is defined as the length of dislocation lines per unit volume of the crystal and is given by eq. (2)

$$\delta = 1/t^2 \qquad (2)$$

where t is the crystallite size.

The ZnO bond length (L) is given by eq. (3),

$$L = \sqrt{\left(\frac{a^2}{3} + \left(\frac{1}{2} - u\right)^2 c^2\right)} \qquad (3)$$

where u is a measure of the amount by which each atom is displaced with respect to the next along the 'c' axis. 'u' is given by equation (4)

$$u = \left(\frac{a^2}{3c^2} + 0.25\right) \qquad (4)$$

Table 3: ZnO Particle size, lattice parameters and bond length of S7and S24 samples using Debye–Scherrer equation

Sr No.	Name of parameter	ZnO Powder Sample S37	ZnO Powder Sample S44
1	**Particle size (t)nm**	5.84	5.45
2	**Lattice parameter a Å**	3.2918	3.3242
3	**Lattice parameter c Å**	5.2672	5.302
4	**c/a**	1.6	1.5950
	V Å³	85.61	
5	**Dislocation density δ (nm)⁻²**	29.32×10^{-3}	33×10^{-3}
6	**ZnO bond length Å**	2.0011	2.0203

The ZnO bond length of S37sample was calculated to be 2.0011 Å and that of S44 was found to be 2.0203 Å (Table 3). Reported ZnO bond length in the unit cell of ZnO and neighboring atoms is 1.9767 Å [24]. The calculated ZnO bond lengths of unit cells were observed to be relatively increased as compared to the reported bond lengths.

(b)Size and Microstrain determination: Williamson–Hall (W–H) plots
(I)Uniform deformation model (UDM)

According to Williamson and Hall, the diffraction line broadening is due to crystallite size and strain contribution. Williamson–Hall equation (5) corresponding to uniform deformation model (UDM) is given as [25],

$$\beta_{hkl}\cos\theta_{hkl} = \frac{K\lambda}{t} + 4\varepsilon\sin\theta_{hkl} \qquad (5)$$
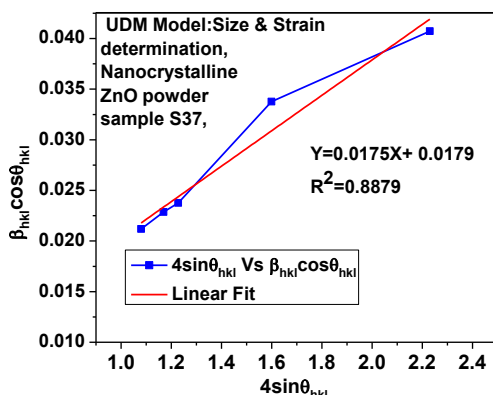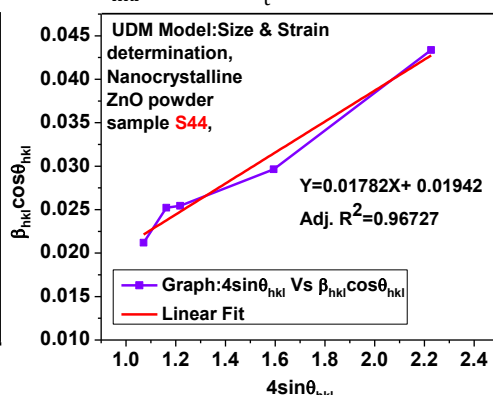

Figure 9(a): Sample S37

Figure 9(b): Sample S44

Figure 9 Plots of $4\sin\theta_{hkl}$ versus $\beta_{hkl}\cos\theta_{hkl}$-UDM model

Figure 9 shows graph of UDM for ZnO nanoparticles. The values of $\beta_{hkl}\cos\theta_{hkl}$ (y-axis) were plotted against $4\sin\theta_{hkl}$ (x-axis). The crystalline size t was estimated from the y-intercept and the microstrain ε was determined from the slope of the linear fit.

Table 4: Particle size and strain determined using W H method- uniform deformation model (UDM)

Name of sample	Particle size nm	Strain ε×10⁻³
S37	7.75	17.5
S44	7.15	17.82

The nanoparticle size and strain ε of S37 and S44 ZnO samples were determined from the graphs in Figures 9(a) and (b) respectively and summarized in Table 4.

(II)Uniform stress deformation model (USDM)

Equation (6) represents the uniform stress deformation model (USDM) of Williamson–Hall equation [25]. It was used to determine size, strain and stress.

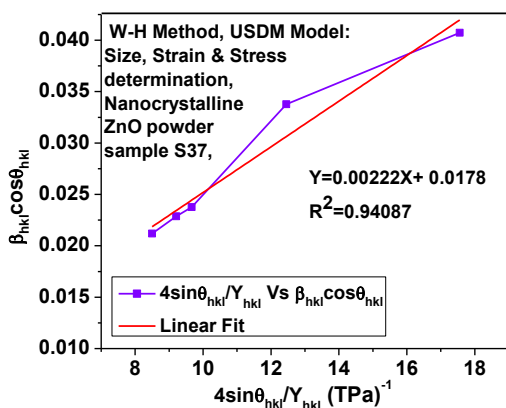$$\beta_{hkl}\cos\theta_{hkl} = \frac{K\lambda}{t} + \frac{4\sigma\sin\theta_{hkl}}{Y_{hkl}} \qquad (6)$$
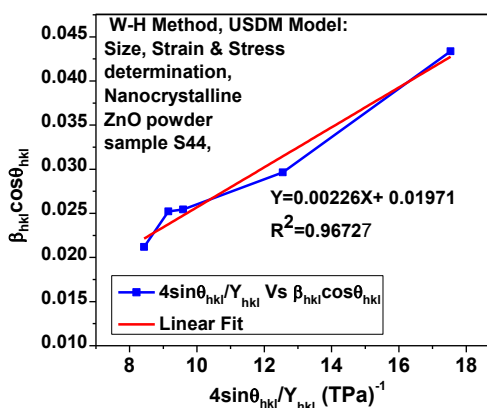
Figure 10(a): Sample S37   **Figure 10(b): Sample S44**

Figure10 Graph of 4sinθ/Y_{hkl} versus $β_{hkl} cosθ_{hkl}$ - USDM model

Values of $β_{hkl} cosθ_{hkl}$ were plotted as a function of $4sinθ/Y_{hkl}$. Figures 10(a) and 10(b) show the graphs of S37 and S44 samples respectively. The uniform deformation stress σ was estimated from the slope of the linear fit and y-intercept gave the crystallite size. Young's modulus, Y_{hkl} ,was calculated to be ~127 GPa. The strain ε of hexagonal ZnO nanoparticles was calculated as the values of stress(σ) and Y_{hkl} were known.

Table 5: Particle size, stress and strain determined using W H method - Uniform stress deformation model (USDM) model

Name of sample	Particle size nm	Stress σ MPa	Strain ε×10^{-3}
S37	7.8	2220	17.48
S44	7.04	2260	17.8

The nanoparticle size, stress σ and strain ε of S37and S44 ZnO samples were determined and summarized in Table 5.

(III)Uniform deformation energy density model (UDEDM)

Uniform deformation energy density model (UDEDM)was used to determine the energy density of a crystal. The equation (7) represents UDEDM model of W-H method. Using relation for energy density $u_{ed} = (ε^2 Y_{hkl})/2$ in equation for UDM model (equation (5)), following equation for UDEDMcan be obtained as [25],

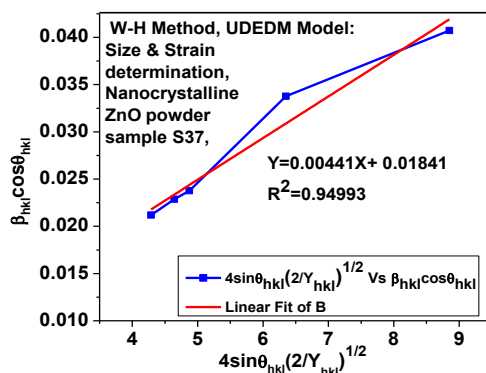$$β_{hkl}cosθ_{hkl} = \frac{Kλ}{t} + 4sinθ_{hkl}\sqrt{2u_{ed}/Y_{hkl}}$$
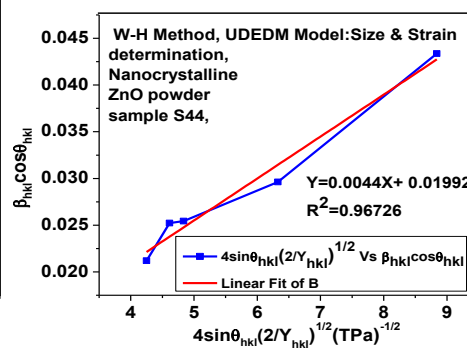
$$(7)$$

Figure 11(a): Sample S37   **Figure 11(b): Sample S44**

Figure 11 Graph of 4sinθ $_{hkl}$ (2/Y_{hkl})$^{1/2}$ versus $β_{hkl} cosθ_{hkl}$ -UDEDM model

Figure 11 shows the plot of $β_{hkl} cosθ_{hkl}$ versus $4sinθ_{hkl} (2/Y_{hk})^{1/2}$. The anisotropic energy density u_{ed} was estimated from the slope of the linear fit and the crystallite size t from the y-intercept. The stress σ was calculated from relation,

$u_{ed} = (σ^2/2Y_{hkl})$ and the lattice strain ε was calculated by using relation, $σ = εY_{hkl}$.

Table 6: Particle size, energy density, stress and strain determined using W H method -UDEDM) model

Name of sample	Particle size nm	Energy Density $u_{ed}MJm^{-3}$	Stress σ MPa	Strain $ε×10^{-3}$
S37	7.54	19.45	1572	12.38
S44	6.97	19.36	1568	12.35

ZnO nanoparticle size, energy density, stress σ and strain ε of S37and S44 samples were determined from the graphs in Figure 11(a) and 11(b) respectively and summarized in Table 6.

3.2.4Microstructural Analysis of ZnO nanoparticle
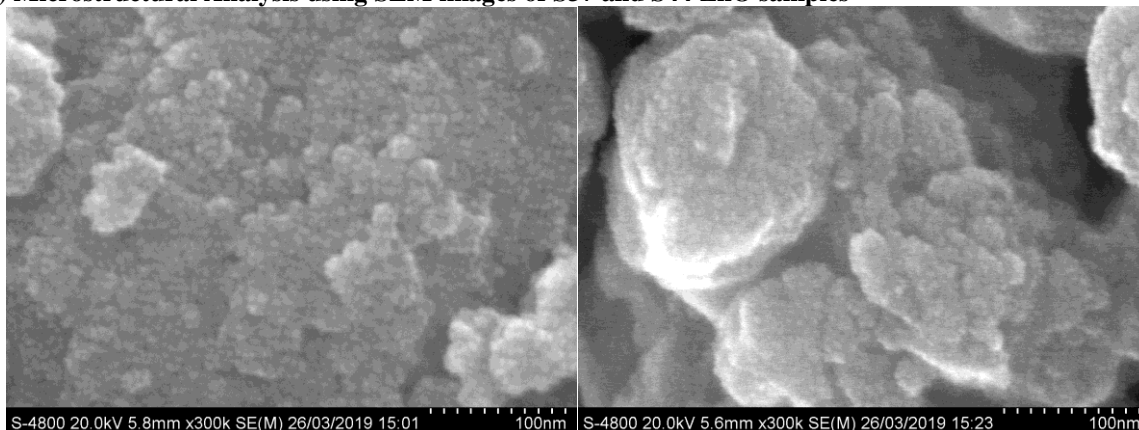**(a) Microstructural Analysis using SEM images of S37 and S44 ZnO samples**

S-4800 20.0kV 5.8mm x300k SE(M) 26/03/2019 15:01 100nm	S-4800 20.0kV 5.6mm x300k SE(M) 26/03/2019 15:23 100nm

Fig.12(a)SEM image of sample S37   **Fig.12(b)SEM image of sample S44**

Figure 12(a) and Figure 12(b) show SEM images of nanocrystalline ZnO powder samples: S37 and S44 respectively. The particle size measured from SEM image of S37 was found to be 8.7 nm and the particle size of S44 was found to be 7.3 nm.

ZnO nanoparticle size, stress σ, strain ε and energy density of S7and S24 samples determined by using Debye Scherrer method, Williamson–Hall (W–H) methods (UDM, USDM and UDEDM models) and from SEM-TEM images are summarized in Table 7.

Table 5: Summary –ZnO Particle size, energy density, stress and strain using Debye-Scherrer Method, W-H methods –UDM, USDM, UDEDM models, SEM and TEM

Sr.no.	Technique used	Particle size nm		Energy Density $u_{ed}MJm^{-3}$		Stress σ MPa		Strain $ε×10^{-3}$	
		S37	S44	S37	S44	S37	S44	S37	S44
1	Debye-Scherrer Method	5.84	5.45	--	--	--	--	--	--
2	W-H method-uniform deformation model (UDM)	7.75	7.15	--	--	--	--	17.5	17.82
3	W-H method-Uniform stress deformation model (USDM)	7.8	7.04	--	--	2220	2260	17.48	17.8
4	W-H method-Uniform deformation energy density model (UDEDM)	7.54	6.97	19.45	19.36	1572	1568	12.38	12.35
5	SEM	8.7	7.3	--	--	--	--	--	--

IV. DISCUSSION

ZnO is brittle material. High energy ball-milling technique is therefore suitable to prepare nanocrystalline ZnO powder. The planet like movement of vial and rotating support disk in ball mill produce centrifugal force. The force acts on powder to be ground and grinding balls. The centrifugal force alternatively acts in like and opposite directions as vial and disk rotate in opposite directions. This causes the friction effect. The powder and grinding balls in motion collide against opposite wall of vial producing the impact effect [22].During high energy milling; the powder particles are repeatedly fractured and welded (on small extent). Whenever two balls collide, some amount of powder is trapped in between them. In case of brittle materials, the tendency to fracture predominates over welding and the rate of decrease of particle size increases. After milling for certain length of time, the temperature in the bowl is relatively larger and state is attained when the rate of fracturing is enhanced, which tends to decrease the average composite particle size. There is tendency to form the particles with an intermediate size from very fine and very large particles. The particle size distribution at this stage is narrow. It is because size of larger particles is reduced below average size and particles smaller than average grow through agglomeration.

The particle size decreases with an increase of milling speed (Figure1). Larger the milling speed, larger would be rotation speed of balls and higher would be the energy input into the milling powder. But maximum milling speed to be employed has limitations. Above the critical speed, the balls would rotate along same track inside of vial and do not fall down to impart force on powder. Therefore, the maximum speed was kept below the critical speed so that the balls fall down from maximum height to impart maximum energy [22, 26]. Smallest particle size was possible by using milling speed of 500 (Figure1) but the milling speed of 300rpm was employed in present investigation to avoid the possibility of rise in temperature and in turn agglomeration of smaller particles. Soft milling conditions were preferred, that is, milling at 300rpm rather than 500rpm was preferred.

The experiments of milling of powder with and without process control agent (PCA) were conducted. Average size of nanoparticles obtained in milling without process control agent (PCA) was observed to be relatively smaller as compared with particle size obtained in milling with PCA (Figure2). Literature reports differ from the observation in present investigations. The milling in presence of PCA would have reduced the friction between powder particles and balls. The reduction in friction would limit fracturing of ZnO particles and would not allow the particle size to be reduced below some critical size.

For same milling time interval, the size of particles in powder milled by balls of smaller diameter was observed to be relatively smaller as shown in Figure 3. The 5 mm diameter balls were observed to be more suitable than 10 and 20 mm balls to get smaller size of ZnO particles (Figure 3). It is reported [22] that the smaller balls produce intense frictional action. The milling conditions such as small ball sizes, lower energies, lower milling speed and lower BPR (soft milling conditions) were observed to be better to get very fine powders. In same weight, balls of smaller diameter would be larger in number as compared with the number of balls having larger diameter. Therefore, overall impact force imparted to ZnO powder by balls of smaller diameter would be larger as compared to the balls of larger diameter resulting into smaller size of particles. In addition to this, ability of the smaller balls to trap powder particles while milling would be larger (as compared with larger balls) as smaller balls form smaller voids in between them.

The optimum BPR (BPR to obtain smallest size of nanoparticles) was observed to be 15:1when the powders were milled by using 10mm or 20mm balls and optimum BPR was observed to be (30:1) when the powders were milled by using 5mm balls (Figure 4). It may be due to larger voids in larger balls and the possibility to escape powder. Though the size of nanoparticles obtained after milling with lager BPR (30:1) is smaller, the amount of nanostructured powder obtained would be smaller while the size of nanoparticles obtained after milling with smaller BPR (15:1) is larger and the amount of nanostructured powder obtained would be larger in amount. Larger the BPR, smaller would be the amount of powder to be milled and in turn smaller would be the amount of powder distributed per ball. The impact of balls on powder particles would therefore be larger or smaller depending upon sizes of balls. For identical milling conditions, the particle size obtained for BPR of 60:1 was observed to be larger as compared to the particle size obtained for BPR of 30:1. The amount distributed per ball in case of BPR of 60:1 may be too low to create optimum impact on powder particles and therefore the particle size would have been found relatively larger.

When the powder was milled for different milling time intervals, the size of nanoparticles decreases with milling time intervals as indicated in Figure5. Some amount of powder is trapped between two balls in motion. The force of impact hardens the particles and they further fracture. If

process of milling is continued for longer interval of time, the powder particles are repeatedly flattened, cold welded, fractured and rewelded. At smaller milling time interval, fracture would dominate welding and rate of decrease in size was observed to be high. At optimum milling time interval, there would be balance between the fracture and welding. The agglomeration forces in ZnO like brittle material are relatively smaller. Therefore, the tendency to reweld and form larger particles is expected to be low.

Present investigators have used ball of different sizes to mill ZnO - the brittle material. But the mixture of balls of different sizes was not found to be advantageous to obtain particles of smaller sizes as compared to the balls of same size to mill the powder (Figure6).The result in present investigation differs from reported [22].

When there is no strain on set of transverse reflecting planes in crystallite, then the interplaner spacing is d. If uniform tensile strain is applied at right angles to the set of transverse reflecting planes in crystallite, the interplaner spacing becomes larger than d and corresponding x ray diffracting peak shifts to lower angles. This peak shift is the basis of XRD method for measurement of macrostress. If the grain is bent and the strain is non-uniform, the interplaner spacing on tension side exceeds d and on compression side it is less than d and somewhere in between it is equal to d[27].

The particle size of sample S37 determined from SEM image was found to be 8.7nm; and particle size of sample S44 determined from SEM image was found to be 7.3 nm. The values of crystallite sizes of S37and S44 samples were also calculated from the W-H analysis which are in agreement (Table 7) with the average sizes of nanoparticles measured from SEM images. The USD, USDM and UDEDM models of W-H plots are observed to be helpful in determining the strain, stress, and energy density values with a certain approximations, and hence, these models are preferable to define the crystal perfection [28-29].

V. CONCLUSIONS

High energy ball milling was observed to be simple and cost effective technique to obtain nanostructured metal oxide semiconducting powders. Monodisperse powder having average particle size smaller up to 5.5nm was produced using this technique. Milling speed of 300 rpm was preferred (Soft milling conditions) to avoid larger heat generation and particle aggregation due to welding at higher milling speed. Under identical milling conditions, the average nanoparticle sizes of the powders milled without PCA were observed to be relatively smaller as compared with average nanoparticle sizes of the powders milled in presence of PCA. The ZnO nanoparticles of smallest size were obtained when powders were milled with balls of 5mm diameter as compared with the particle sizes in powders milled with balls of diameters 10 and 20 mm. For very small BPR (3.5:1), the smallest particle size was possible when balls of 10mm were used instead of 5mm. The particle size was observed to be decreasing with milling time interval, reached to minimum and was then remains nearly same with further increase of milling time. The particle size was observed to be decreasing fastly with BPR, reached to minimum at BPR of 30:1 and was increased with further increase of BPR when milling was conducted by using 5mm balls. Average size of nanoparticle obtained by milling with 5mm was observed to be smaller than the size of nanoparticles obtained by milling with 10mm and average size of nanoparticle obtained by milling with 10mm was observed to be smaller than the size of nanoparticles obtained by milling with 20mm balls. The milling with mixture of balls of different diameters was not found to be beneficial to get smallest size of nanoparticles as compared to the smallest size of nanoparticles obtained after milling with 5mm balls. The peak broadening (FWHM) of XRD patterns was observed to be increasing with the decrease in size of nanoparticles. Debye Scherrer method and Williamson and Hall methods (UDM, USDM and UDEDM models) were used to determine size, strain, stress and energy density associated with nanoparticles with a certain approximations. The values of crystallite sizes associated ZnO samples calculated from the W-H analysis were in agreement with the average sizes of nanoparticles measured from SEM images.

The lattice contractions were observed with decreasing particle size. This observation strongly indicates that surface tension plays a major role in determining lattice parameters. Decrease of anion vacancy defects and internal stress in smaller particles may also be the reasons of contraction in lattice constants of unit cells.

REFERENCES

[1]. S. Sakohara, M. Ishida, M.A.Anderson, J. Phys. Chem. B 102(1998) 10169–10175.

[2]. S.Hingorani, V. Pillai, P.Kumar,M.S. Muntai, D.O.Shah, Mater. Res. Bull. 28(1993)1303–1310.

[3]. X.Zhao, S.C.Zhang, C. Li, B. Zheng, H. Gu, J. Mater. Synth. Process. 5(1997) 227.

[4]. X. Bai, L. Li, H. Liu, L. Tan, T. Liu, and X. Meng, ACS Appl Mater Interfaces, vol. 7, no. 2, pp. (2015)1308–1317.

[5]. M.Moritz , M. Geszke-Moritz, Chemical Engineering Journal, vol. 228, (2013) pp. 596–613.

[6]. L.A.Patil, A.R.Bari, M.D.Shinde, V.V.Deo, M.P.Kaushik,Sensors and Actuators B: Chemical, 161(2012)372-380.

[7]. W. J. Jeong, S. K. Kim, and G. C. Park, Thin Solid Films, vol. 506-507 (2006)pp. 180–183.

[8]. A. A. Reinert, C. Payne, L. Wang, J. Ciston, Y. Zhu, and P. G. Khalifah, Inorganic Chemistry, vol. 52, no. 15, pp. (2013)8389–8398.

[9]. K. Rekha, M. Nirmala, M. G. Nair, and A. Anukaliani, Physica B: Condensed Matter, vol. 405, no. 15, (2010)3180–3185.

[10]. S. Nair, A. Sasidharan, V. V. Divya Rani et al., Journal of Materials Science: Materials in Medicine, vol. 20, no. 1, (2009)S235–S241.

[11]. D.R.Patil, L.A.Patil,Sensors and Actuators B: Chemical 123, (2007)546-553.

[12]. W. W. Adams and R. H. Baughman, Richard E. Smalley (1943–2005), Science, vol. 310, no. 5756, (2005)1916.

[13]. M. Nasrollahzadeh and S.MohammadSajadi, Journal of Colloid and Interface Science, vol. 457, (2015)141–147.

[14]. S. Sabir, M. Arshad, and S. K. Chaudhari, The Scientific World Journal, vol. 2014,(2014)Article ID925494.

[15]. X. Wang, Y.Ding, C. J. Summers, and Z. L. Wang, The Journal of Physical Chemistry B, vol. 108, no. 26, (2004)8773–8777.

[16]. P.-J. Lu, S.-C. Huang, Y.-P. Chen, L.-C. Chiueh, and D. Y.-C. Shih, Journal of Food and Drug Analysis, vol. 23, no. 3, (2015)587–594.

[17]. M. J. Osmond and M. J. McCall, Nanotoxicology, vol. 4, no. 1 (2010)15–41, 2010.

[18]. B. Baroli, Journal of Pharmaceutical Sciences, vol. 99, no. 1,(2010)21–50.

[19]. M. E. Darvin, S. F. Haag, J. Lademann, L. Zastrow, W. Sterry, and M. C. Meinke, Journal of Investigative Dermatology, vol. 130, no. 2(2010) 629–631.

[20]. J. Liu, C. Guo, C. M. Li et al., Electrochemistry Communications, vol. 11, no. 1, (2009)202–205.

[21]. L.A. Patil, A.R. Bari, M.D. Shinde and Vinita Deo, Journal of Experimental Nanoscience Vol. 6, No. 3, June 2011, 311–323

[22]. C. Suryanarayana, Progress in Material Science, 46(2001)1-184.

[23]. G. K. Williamson, W. H. Hall, Acta Metall. 1 (1953) 22-31.

[24]. U.Seetawan, S.Jugsujinda, T.Seetawan, A. Ratchasin, C.Euvananont, C. Junin, C. Thanachayanont, P. Chainaronk, Maters. Sci. Appls. 2, (2011)1302–1306.

[25]. T.Pandiyarajan, B. Karthikeyan ,Optical, J. Nanopart. Res. 14(2012) 647.

[26]. A.Calka, AP.Radlinski, Mater. Sci and Engng. A134(1991) 1350-1353

[27]. A.Khorsand Zak, W.H.Abd.Majid, M.E.Abrishami, RaminYoysefi, Solid State Sciences 13 (20111)251-256.

[28]. P. Bindu, S.Thomas,Journal of Theoretical and Applied Physics, 8 (4) (2014,) 123–134

[29]. M.Saleem, L. Fang, H.B. Ruan, F. Wu, Q.L.Huang, C.L. Xu, C.Y. Kong,Intl. J. Phy. Sci. 7(23) (2012) 2971–2979